Inorg. Chem. **2008**, *47*, 3603−3609

Synthesis, Structure, and Optical Properties of the Quaternary Seleno-gallates $NaLnGa_4Se_8$ (*Ln* = La, Ce, Nd) and Their Comparison with the Isostructural Thio-gallates

Amitava Choudhury and Peter K. Dorhout*

Department of Chemistry, Colorado State University, Fort Collins, Colorado 80523

Received October 8, 2007

Three new quaternary seleno-gallates containing rare-earth metals and sodium cations, have been synthesized by a solid-state route in evacuated quartz ampoules: $NaLnGa_4Se_8$ (*Ln* = La(**I**), Ce (**II**) and Nd (**III**)). The synthesis involved the stoichiometric combination of sodium polyselenides, rare-earth metal, Ga_2Se_3, and Se or elemental Ga in place of Ga_2Se_3. Single-crystal structure analysis indicated that the compounds are isostructural to the thio-analogue, $NaNdGa_4S_8$. The structures of **I**−**III** are described in terms of layers of $GaSe_4$ tetrahedra joined by corner- and edge-sharing; the alkali-metal cations and the trivalent rare-earth metal cations occupy square antiprismatic sites between the layers. The optical properties of the compounds have been investigated and compared with the isostructural thio-gallate. The band gap of **I** was located around 2.65 eV. The band gaps of **II** and **III** were 2.66 and 2.73 eV, respectively, considerably narrower than their thio-analogues (∼3.4 eV). The contraction of the band gap was attributed to the shift of the valence band to higher energy due to the involvement of higher energy (4p) Se orbitals. The 4f → 5d gap of **II** is found to be located around 2.32 eV, which is 0.26 eV narrower than the thio-analogue is due to a greater dispersion of the *Ln*-(5d) band caused by more covalent Ce-Se bonds as well as rising of the f level energy.

Introduction

The chemistry of rare-earth metals in a chalcogenide matrix, both in crystalline and glassy forms, constitutes an important area of research. Rare-earth metal chalcogenides, in combination with a main group element, not only present a rich structural chemistry[1] but also a wide variety of physical properties mainly useful in optical and magneto-optical devices.[2] The excellent optical properties of rare earth chalcogenides are related to the effect of the rare-earth metal, which has inner lying f-orbitals with localized energy levels and narrow optical absorption and emission bands combined with the effect of high covalency, high refractive index, and low energy of phonons of the heavy chalcogen atoms.[3,4] However, multiphonon relaxation can significantly reduce the quantum efficiency of luminescence. In solids with smaller phonon energies, the probability of multiphonon relaxation is lowered; at the same, the time quantum efficiency of luminescence can be higher. Also, some of the mid-IR transitions that are normally quenched in the larger phonon energy hosts like oxides or fluorides become active in chalcogenide hosts.[4] For these reasons, rare-earth metal chalcogenides have been investigated as phosphors both in crystalline[5–14] and glassy matrices.[15] Many of these com-

* To whom correspondence should be addressed. Fax: (970) 491-1801. E-mail: pkd@lamar.colostate.edu.

(1) (a) Wu, P.; Ibers, J. A. *J. Alloys Compd.* **1995**, *229*, 206. (b) Sheldrick, W. S.; Wachhold, M. *Coord. Chem. Rev.* **1998**, *176*, 211. (c) Mitchell, K.; Ibers, J. A. *Chem. Rev.* **2002**, *102*, 1929.
(2) Kumta, P. N.; Risbud, S. H. *J. Mater. Sci.* **1994**, *29*, 1135.
(3) (a) *Spectroscopic Properties of Rare Earths in Optical Materials*; Liu, G.; Jacquier, B., Eds.; Tsinghua University Press and Springer-Verlag Berlin: Tsinghua, 2005; Vol. *83*. (b) Cotton, S. *Lanthanide and Actinide Chemistry*; John Wiley & Sons.: Chichester, U.K., 2006.
(4) (a) Reisfeld, R.; Bornstein, A. *Chem. Phys. Lett.* **1977**, *47*, 194. (b) Reisfeld, R.; Bornstein, A.; Flahaut, J.; Loireau-Lazac'h, A. M. *The Rare Earths in Modern Science Technology*; McCarthy, G. J., Rhyne, J. J., Silber, H. B., Eds.; Plenum: New York, 1980; Vol. 2. (c) Reisfeld, R. *Ann. Chim. Fr.* 1982, *7*, 147.
(5) (a) Peters, T. E.; Baglio, J. A. *J. Electrochem. Soc.* **1972**, *119*, 230. (b) Peters, T. E. *J. Electrochem. Soc.* **1972**, *119*, 1720.
(6) (a) Garcia, A.; Fouassier, C; Dougier, P. *J. Electrochem. Soc.* **1982**, *129*, 2063. (b) Ibañez, R.; Garcia, A.; Fouassier, C.; Hagenmuller, P. *J. Solid State Chem.* **1984**, *53*, 406. (c) Ibañez, R.; Gravereau, P.; Garcia, A.; Fouassier, C. *J. Solid State Chem.* **1988**, *73*, 252. (d) Davolos, M. R.; Garcia, A.; Fouassier, C.; Hagenmuller, P. *J. Solid State Chem.* **1989**, *83*, 316.
(7) Benalloul, P.; Barthou, C.; Benoit, J.; Eichenauer, L.; Zeinert, A. *Appl. Phys. Lett.* **1993**, *63*, 1954.

10.1021/ic701986j CCC: $40.75
Published on Web 03/15/2008

pounds are important industrial pigments.[16] Among the chalcogenides, one of the most studied systems is MGa_2S_4 (M = Ca, Sr, Ba) doped with various rare-earth metals, MGa_2S_4:Ln^{2+}/Ln^{3+}, or sometimes charge-compensated by an alkali-metal cation, as in MGa_2S_4:Ln^{3+}/Na^+, generating an important class of phosphors for many luminescence applications.[5–13] The structures of MGa_2S_4 (M = Ca, Sr, Ba) have been determined from single-crystal X-ray studies, which indicated that MGa_2S_4 phases (M = Ca, Sr) crystallized in the orthorhombic system with space group *Fddd*,[17] whereas $BaGa_2S_4$ crystallized in the cubic system with space group *Pa*3.[18] After the first report by Peters and Baglio that MGa_2S_4:Ce,Na or MGa_2S_4:Eu phosphors can fluoresce strongly under UV and cathode rays,[5] there have been several important discoveries in these systems. For example, a bright blue emission from thin films of MGa_2S_4:Ce^{3+} (M = Ca, Sr) may afford full color electroluminescent displays.[8,9] Similarly, $SrGa_2S_4$:Eu^{2+} films emit saturated green light.[7,10] Evidence of lasing has also been observed in $CaGa_2S_4$:Eu^{2+} (2.19 eV)[12] and $CaGa_2S_4$:Dy^{3+} (mid-IR, 4.3 μm).[13] Another interesting feature about this host was its ability to take up increased levels of Ln^{3+} doping when the charge is compensated by Na^+ cations, as in $Na_xLn_x(M_{1-2x})Ga_2S_4$, with much lower concentration quenching and fewer defects in the structure.[6b,c] Thus, in the limit composition of x = 0.5 in $Na_xLn_x(M_{1-2x})Ga_2S_4$, stoichiometric quaternary sulfides of the composition $NaLnGa_4S_8$ (Ln = Ce, Nd) may be obtained, where the alkaline earth metal has been entirely substituted by a combination of the trivalent rare-earth and the monovalent alkali metals.[5,6c,9c] The structure of $NaNdGa_4S_8$ has been determined and is isostructural to MGa_2S_4 (M = Ca, Sr).[6c,17] However, until now, there have been only few reports of a selenium analogue of these compounds except for a brief report on $CaGa_2Se_4$:Eu.[18] In this regard, we wanted to prepare and study the stoichiometric composition $NaLnGa_4Se_8$ (Ln = La, Ce, Nd) and determine their structures and optical properties. The replacement of S^{2-} by Se^{2-} will likely alter the absorption and emission properties, which depend on the ligand field strength and the extent of covalency in the bonding as well as the substitutional effect on the f → d transition of Ce^{3+} and f→ f transition of Nd^{3+}, which is one of the most studied rare-earth metals for its use in solid state lasers.[19]

Experimental Section

Synthesis. The compounds were prepared by the stoichiometric reaction of elemental Se, lanthanide metal, and the binary compounds Ga_2Se_3 and alkali-metal selenide (Na_2Se_2 or Na_2Se) or by the reaction of elemental Se, lanthanide metal, and gallium metal with the binary Na_2Se. Gallium ingots (99.999%, Cerac), Se (99.999%, Johnson-Mathey), La (shavings from a rod, 99.9%, Alfa Aesar), Ce (Alfa Aesar, 99.9% powder), Nd (99.99%, 40 mesh, Cerac), and Na_2Se (60 mesh, Cerac) were used as received and Na_2Se_2 and its sulfide counterpart were prepared from the stoichiometric combination of the elements in liquid ammonia as described elsewhere.[20,21] Reactants were loaded into fused-silica ampoules inside a N_2-filled glovebox. The ampoules were flame-sealed under vacuum and placed in a temperature-controlled furnace. The furnace was ramped to 850−900 °C at a rate of 35 °C/h and held constant at that temperature for several hours to days. The furnace was then slowly cooled to ambient temperature at a rate of 5 °C/h. The details of the reactions are given in Table 1. Good-quality crystals for the single-crystal X-ray analyses were obtained from all the reactions, with the largest yields resulting from those where the Ga source was Ga_2Se_3. The color of the single crystal of **I** was light amber, those of Ce- (**II**) and Nd-containing (**III**) compounds were red;

(8) (a) Barrow, W. A.; Coovert, R. E.; Dickey, E.; King, C. N.; Laakso, C.; Sun, S.-S.; Tuenge, R. T.; Wentross, R. C.; Kane, J. *Society of Information Display International Symposium Digest of Technical Papers*; Society of Information Display: Playa del Rey, CA, 1993; p 761. (b) Sun, S.-S.; Tuenge, R. T.; Kane, J.; Ling, M. *J. Electrochem. Soc.* **1994**, *141*, 2877.

(9) (a) Tanaka, K.; Inoue, Y.; Okamoto, S.; Kobayashi, K. *J. Cryst. Growth* **1995**, *150*, 1211. (b) Inoue, Y.; Tanaka, K.; Okamoto, S.; Kobayashi, K.; Fujimoto, I. *Jpn. J. Appl. Phys.* **1995**, *34*, L180. (c) Inoue, Y.; Kobayashi, K.; Tanaka, K.; Okamoto, S.; Tsuchiya, Y.; Takizawa, K. *IEEE Trans. Broadcasting* **1996**, *42*, 259. (d) Tanaka, K.; Inoue, Y.; Okamoto, S.; Kobayashi, K.; Takizawa, K. *Jpn. J. Appl. Phys.* **1997**, *36*, 3517. (e) Ronot-Limousin, I.; Garcia, A.; Fouassier, C.; Barthou, C.; Benalloul, P.; Benoit, J. *J. Electrochem. Soc.* **1997**, *144*, 687. (f) Zhang, F.-L.; Yang, S.; Stoffers, C.; Penczek, J.; Yocom, P. N.; Zaremba, D.; Wagner, B. K.; Summers, C. J *Appl. Phys. Lett.* **1998**, *72*, 2226.

(10) (a) Yang, S.; Stoffers, C.; Zhang, F.; Jacobsen, S. M.; Wagner, B. K.; Summers, C. J.; Yocom, N. *Appl. Phys. Lett.* **1998**, *72*, 158. (b) Benalloul, P.; Barthou, C.; Benoit, J. *J. Alloys Compd.* **1998**, *275–277*, 709.

(11) (a) Georgobiani, A. N.; Gruzintsev, A. N.; Barthou, C.; Benalloul, P.; Benoit, J.; Tagiev, B. G.; Tagiev, O. B.; Dzhabborov, R. B. *J. Electrochem. Soc.* **2001**, *148*, H167. (b) Hidaka, C.; Takizawa, T. *J. Cryst. Growth* **2002**, *237–239*, 2009. (c) Bealloul, P.; Barthou, C.; Fouassier, C.; Georgobiani, A. N.; Lepnev, L. S.; Emirov, Y. N.; Gruzintsev, A. N.; Tagiev, B. G.; Tagiev, O. B.; Jabbarov, R. B. *J. Electrochem. Soc.* **2003**, *150*, G62. (d) Kato, A.; Yamazaki, M.; Najafov, H.; Iwai, K.; Bayramov, A.; Hidaka, C.; Takizawa, T.; Iida, S. *J. Phys. Chem. Solids* **2003**, *64*, 1511. (e) Iida, S.; Kato, A.; Tanaka, M.; Najafov, H.; Ikuno, H. *J. Phys. Chem. Solids* **2003**, *64*, 1815. (f) Bessière, A.; Dorenbos, P.; van Eijk, C. W. E.; Yamagishi, E.; Hidaka, C.; Takizawa, T. *J. Electrochem. Soc.* **2004**, *151*, H254. (g) Chartier, C.; Barthou, C.; Benalloul, P.; Frigerio, J. M. *J. Lumin.* **2005**, *111*, 147. (h) Jabbarov, R. B.; Chartier, C.; Tagiev, B. G.; Tagiev, O. B.; Musayeva, N. N.; Barthou, C.; Benalloul, P. *J. Phys. Chem. Solids* **2005**, *66*, 1049. (i) Dorenbos, P. *J. Lumin.* **2007**, *122–123*, 315.

(12) Iida, S; Matsumoto, T.; Mamedov, N. T.; An, G.; Maruyama, Y.; Bairamov, A. I.; Tagiev, B. G.; Tagiev, O. B.; Dzhabbarov, R. B. *Jpn. J. Appl. Phys., Part 2* **1997**, *36*, L857.

(13) Nostrand, M. C.; Page, R. H.; Payne, S. A.; Krupke, W. F.; Schunemann, P. G. *Opt. Lett.* **1999**, *24*, 1215.

(14) (a) Riccardi, R.; Gout, D.; Gauthier, G.; Guillen, F.; Jobic, S.; Garcia, A.; Guguenin, D.; Macaudière, P.; Fouassier, C.; Brec, R. *J. Solid State Chem.* **1999**, *147*, 259. (b) Gauthier, G.; Jobic, S.; Evain, M.; Koo, H.-J.; Whangbo, M.-H.; Fouassier, C.; Brec, R. *Chem. Mater.* **2003**, *15*, 828.

(15) (a) Viana, B.; Palazzi, M.; LeFol, O. *J. Non-Cryst. Solids* **1997**, *215*, 96. (b) Kadono, K.; Shojiya, M.; Takahashi, M.; Higuchi, H.; Kawamoto, Y. *J. Non-Cryst. Solids* **1999**, *259*, 39. (c) Tver'yanovich, Y. S.; Degtyarev, S. V.; Pivovarov, S. S.; Smirnov, V. B.; Kurochkin, A. V. *J. Non-Cryst. Solids* **1999**, *256–257*, 95. (d) Lima, S. M.; Sampaio, J. A.; Catunda, T.; de Camargo, A. S. S.; Nunes, L. A. O.; Baesso, M. L.; Hewak, D. W. *J. Non-Cryst. Solids* **2001**, *284*, 274.

(16) Gauthier, G.; Jobic, S.; Boucher, F.; Macaudière, P.; Huguenin, D.; Rouxel, J.; Brec, R. *Chem. Mater.* **1998**, *10*, 2341.

(17) Eisenmann, B.; Jakowski, M.; Klee, W.; Schaefer, H. *Rev. Chim. Miner.* **1983**, *20*, 255.

(18) Donahue, P. C.; Hanlon, J. E. *J. Electrochem. Soc.* **1974**, *121*, 230.

(19) Kaminskii, A. A. *Laser Crystals*, 2nd ed.; MacAdam, D. L., Ed.; Springer Series in Pptical Sciences Vol. 14;Springer-Verlag: Berlin, 1990.

(20) (a) Schewe-Miller, I. *Metallreiche Hauptgruppenmetall-Chalkogenverbindungen: Synthese, Strukturen und Eigenschafte*. Ph.D. Thesis, Max-Planck-Institut für Festkörperforschung, Stuttgart, Germany, 1990. (b) Liao, J.-H.; Kanatzidis, M. G. *Inorg. Chem.* **1992**, *31*, 431.

(21) Stoichiometric quantities of metallic Na and S were reacted in liquid ammonia in a flask in closed Schlenk lines similar to the synthesis of Na_2Se_2 reported in ref 20b.

Table 1. Molar Ratios of the Starting Reactants and Synthesis Parameters for the Quaternary Chalcogenides, $NaLnGa_4Q_8$ (Ln = La, Ce, Nd; Q = S, Se)

	reactants				T (°C)	time (h)
I	Na_2Se (6.2) [a]	2 La (13.9)	4 Ga_2Se_3 (75.3)	3 Se (11.8)	850	96
I	Na_2Se (62.5)	2 Ce (138.9)	8 Ga (278.9)	15 Se (592.2)	850	96
II	Na_2Se (10)	2 Ce (22.4)	4 Ga_2Se_3 (120.4)	3 Se (18.9)	850	120
II	Na_2Se_2 (8.2)	2 Ce (11.2)	4 Ga_2Se_3 (60.2)	2 Se (6.3)	850	72
II	Na_2Se (62.5)	2 Ce (140.1)	8 Ga (278.9)	15 Se (592.2)	900 and 700	5 and 120 [b]
III	Na_2Se (62.5)	2 Nd (144.2)	8 Ga (278.9)	15 Se (592.2)	900 and 700	5 and 120 [b]
III	Na_2Se_2 (20.3)	2 Nd (28.7)	4 Ga_2Se_3 (150)	2 Se (157)	850	96
c	Na_2S_4 (13.9)	2 Ce (22.4)	4 Ga_2S_3 (75.4)		850	120
d	Na_2S_4 (13.9)	2 Nd (23.1)	4 Ga_2S_3 (75.4)		850	120

[a] The numbers in the parentheses indicate absolute quantities of the reactants in milligrams. [b] The ampule was heated at 900 °C for 5 h and then cooled to 700 °C with 10 °C/h and annealed at that temperature for 120 h. c, $NaCeGa_4S_8$; d, $NaNdGa_4S_8$.

however, the colors of the finely ground powder of the compounds **I** and **II** were beige, whereas that of **III** is slightly darker and looks more beige-brown (see the Supporting Information, Figure S1). The powder X-ray diffraction (PXRD) of the as-synthesized product for all the reactions indicated a minor amount of $NaGa_3Se_5$ as an impurity. We have also synthesized the thio-analogues of $NaLnGa_4Se_8$ (Ln = Ce, Nd) employing a new synthetic strategy similar to the selenides, but different from the previously reported methods, which involve sulfidizing the oxides by flowing H_2S or CS_2.[5,6a–d,9e] Our method involves the sealed-tube reaction of the stoichiometric combination of Na_2S_4, Ln (Ln = Ce, Nd) and Ga_2S_3 at 850 °C for 120 h as given in Table 1. The PXRD of the as synthesized products indicated the formation of pure $NaCeGa_4S_8$ and $NaNdGa_4S_8$ as compared to the previously reported patterns for the two compounds.[5,6c]

Single-Crystal X-ray Diffraction. Intensity data sets for the compound **I** was collected on a Bruker APEX II, whereas data sets for **II** and **III** were collected on Bruker Smart CCD diffractometer. These data were integrated with SAINT,[22] the program SADABS was used for absorption correction.[23] The structures were solved by direct methods using SHELXS-97[24] and difference Fourier syntheses. Full-matrix least-squares refinement against F^2 was carried out using the SHELXTL-PLUS[25] suit of programs. On the basis of the systematic absences, space group *Fddd* was chosen for both compounds, which immediately revealed that **I**−**III** are isostructural to the sulfide analogue $NaNdGa_4S_8$.[6c] Rare-earth metal cations can be easily located on 8*a* and 8*b* sites, whereas subsequent refinement identified Na on the 16*e* site and two Ga and four Se on the 32*h* site. The last cycles of refinement for **I**−**III** included anisotropic thermal parameter refinement for all the atoms. Details of the final refinements and the cell parameters for **I**−**III** are given in Table 2. The final atomic coordinates and important interatomic distances and angles for **I**−**III** are given in Tables 3 and 4, respectively.

UV–Vis Spectroscopy. Diffuse reflectance measurements were taken on a Varian Cary 500 Scan UV–vis-NIR spectrophotometer equipped with a Praying Mantis accessory. A Teflon standard was used as a reference. The Kubelka–Munk function was applied to obtain band gap information.[26] The band gap was determined as the intersection point between the energy axis at the absorption–offset and the line extrapolated from the linear portion of the absorption edge in the $K-M$ function vs energy plot.

Table 2. Crystal Data and Structural Refinement Parameters for Compounds **I**−**III**

	I	II	III
chemical formula	$NaLaGa_4Se_8$	$NaCeGa_4Se_8$	$NaNdGa_4Se_8$
fw	1072.46	1073.69	1077.79
space group	*Fddd* (No. 70)	*Fddd* (No. 70)	*Fddd* (No. 70)
T (K)	296	293	293
wavelength (Å)	0.71073	0.71073	0.71073
a (Å)	21.1979(4)	21.141(1)	21.015(2)
b (Å)	21.1625(7)	21.138(1)	21.045(1)
c (Å)	12.7216(7)	12.712(1)	12.709(1)
$\alpha = \beta = \gamma$ (deg)	90	90	90
V (Å^3)	5706.9(4)	5681.1(8)	5620.8(9)
Z	16	16	16
ρ_{calcd} (Mg m^{-3})	4.993	5.021	5.095
μ (mm^{-1})	30.783	31.12	31.91
R [$I > 2\sigma(I)$][a]	0.0450	0.0281	0.0369
wR (F^2)(all data) [b]	0.1220	0.0596	0.0744

[a] $R_1 = \sum||F_o| - |F_c||/\sum|F_o|$. [b] $wR_2 = \{\sum[w(F_o^2 - F_c^2)^2/\sum[w(F_o^2)^2]\}^{1/2}$, $w = 1/[\sigma^2(F_o)^2 + (aP)^2 + bp]$, where $p = [F_o^2 + 2F_c^2]/3$; $a = 0.0511$ and $b = 71.7748$ for **I**; $a = 0.0271$ and $b = 0$ for **II**; $a = 0.0287$ and $b = 13.261$ for **III**.

Results and Discussion

Structure Description of $NaLnGa_4Se_8$ (Ln = La, Ce, Nd). The structure of $NaLnGa_4Se_8$ can be considered as being assembled from $LnSe_8$ square antiprisms and $GaSe_4$ tetrahedra. The $GaSe_4$ tetrahedra form a layer parallel to the [100] plane through edge- and corner-sharing (Figure 1). Such layers are stacked along the *a*-axis and held together by rare-earth metal and alkali-metal cations that reside between the layers, through the shorter Ln−Se and longer Na−Se bonds, respectively, to form a three-dimensional structure (Figure 2). There are two crystallographically independent Ga atoms, each surrounded by four Se atoms in a tetrahedral environment. Each $GaSe_4$ tetrahedron shares one edge and two corners with the neighboring $GaSe_4$ tetrahedra, as well as $LnSe_8$, and $NaSe_8$ square antiprisms, respectively. The Ga−Se distances are in the range from 2.371(2) to 2.431(1) Å and 2.380(1) to 2.431(2) Å for Ga1 and Ga2, respectively, in compound **I**, 2.3756(7) to 2.4348(7) Å and 2.3792 to 2.4367 Å for Ga1 and Ga2, respectively, in compound **II**, and 2.3734(9) to 2.4343(10) Å and 2.3795(10) to 2.4350(10) Å for Ga1 and Ga2, respectively, in compound **III**. The Se−Ga−Se angles are in the range 97.75(5)–101.77(5)° and 98.56(5)–101.86(5)° for Ga1 and Ga2, respectively, in **I**, 97.88(2)−121.18(2)° and 98.65(2)−124.89(3)° for Ga1 and

(22) *SAINT: Data Processing Software for the SMART System*; Bruker Analytical X-ray Instruments, Inc.; Madison, WI, 1995.
(23) Sheldrick, G. M. *SADABS*; University of Göttingen: Göttingen, Germany, 1997.
(24) Sheldrick, G. M. *SHELXS-97, Programs for X-ray Crystal Structure Solution*; University of Göttingen: Göttingen, Germany, 1997.
(25) Sheldrick, G. M. *SHELXL-97, Programs for X-ray Crystal Structure Refinement*; University of Göttingen: Göttingen, Germany, 1997.
(26) (a) Wendlandt, W. W.; Hecht, H. G. *Reflectance Spectroscopy*; Interscience Publishers: New York, 1966. (b) Kotum, G. *Reflectance Spectroscopy*; Springer-Verlag: New York, 1969.

Table 3. Final Coordinates and Equivalent Isotropic Displacement Parameters of the Atoms for Compounds **I**−**III**

atoms	Wyckoff Site	*x*	*y*	*z*	U_{eq} (Å^2)[a]
		I			
La1	8*a*	1/8	1/8	1/8	0.0105(3)
La2	8*b*	1/8	1/8	5/8	0.0110(3)
Na1	16*e*	0.3780(3)	1/8	1/8	0.0250(19)
Ga1	32*h*	0.75230(5)	0.48980(5)	0.12572(9)	0.0122(3)
Ga2	32*h*	0.74980(5)	0.69498(5)	0.41592(9)	0.0121(3)
Se1	32*h*	0.00160(5)	0.59236(5)	0.24894(8)	0.0124(3)
Se2	32*h*	0.75181(5)	0.58347(4)	0.01509(8)	0.0108(3)
Se3	32*h*	0.58620(5)	0.74879(4)	0.24561(7)	0.0119(3)
Se4	32*h*	0.91335(5)	0.49871(4)	0.99849(7)	0.0116(3)
		II			
Ce1	8*a*	1/8	1/8	1/8	0.0105(1)
Ce2	8*b*	1/8	1/8	5/8	0.0108(1)
Na1	16*e*	0.37804(13)	1/8	1/8	0.0284(10)
Ga1	32*h*	0.75240(2)	0.48979(2)	0.12577(4)	0.0117(2)
Ga2	32*h*	0.74950(2)	0.69497(2)	0.41580(4)	0.0119(2)
Se1	32*h*	0.00222(2)	0.59229(2)	0.24813(3)	0.0125(1)
Se2	32*h*	0.75129(2)	0.58380(2)	0.01511(3)	0.0109(1)
Se3	32*h*	0.58653(2)	0.74841(2)	0.24527(3)	0.0117(2)
Se4	32*h*	0.91302(2)	0.49841(2)	0.99771(3)	0.0115(2)
		III			
Nd1	8*a*	1/8	1/8	1/8	0.0107(2)
Nd2	8*b*	1/8	1/8	5/8	0.0111(2)
Na1	16*e*	0.3783(2)	1/8	1/8	0.0330(17)
Ga1	32*h*	0.75261(3)	0.48979(3)	0.12577(5)	0.0116(2)
Ga2	32*h*	0.74920(4)	0.69512(3)	0.41545(5)	0.0116(2)
Se1	32*h*	0.00317(3)	0.59235(3)	0.24783(5)	0.0126(2)
Se2	32*h*	0.75058(3)	0.58428(3)	0.01533(5)	0.0109(2)
Se3	32*h*	0.58693(3)	0.74786(3)	0.24465(4)	0.0120(2)
Se4	32*h*	0.91259(3)	0.49807(3)	0.99661(4)	0.0115(2)

[a] U_{eq} = 1/3 of the trace of the orthogonalized *U* tensor.

Ga2, respectively, in **II** and 97.83(3)−120.84(4)° and 97.83(3)−125.27(4)° for Ga1 and Ga2, respectively, in **III**. These Se−Ga−Se angles indicate that the $GaSe_4$ tetrahedra are fairly distorted. The cause of distortions can be attributed to the stronger cation–cation repulsions for polyhedra connected by edges than polyhedra connected by vertices, as already been discussed in the case of the sulfide analogue, $NaNdGa_4S_8$.[6c] For example, to reduce the Ga−Ga repulsion through the edge, the Se−Ga−Se angles have to be more acute (97.75−98.71°).

There are two crystallographically independent rare-earth metal atoms in the structure of $NaLnGa_4Se_8$ (*Ln* = La, Ce, and Nd), where each rare-earth cation is surrounded by eight Se^{2-} anions in a slightly distorted square-antiprismatic environment. Each $LnSe_8$ polyhedron is connected to four $GaSe_4$ tetrahedra and two $NaSe_8$ square antiprisms through edge-sharing and eight $GaSe_4$ and four $NaSe_8$ polyhedra through common vertices. There are no *Ln*−Se−*Ln* linkages in the structure, indicating that the $LnSe_8$ square antiprisms are isolated from each other and the distance between two rare-earth metal cations is 6.360(2), 6.356(1), and 6.355(1) Å for La, Ce, and Nd, respectively (Figure 3). Ibanez et al. has attributed low concentration quenching of luminescence in the sulfide analogue of the Nd compound, $NaNdGa_4S_8$, to the long distance between the rare-earth metal cations.[6c] As the distance between the rare-earth metal cations increases, the repulsion, as well as the probability of the various mechanisms responsible for the nonradiative losses, is also decreased. The La−Se, Ce−Se, and Nd−Se distances are in the range 3.1313(10)–3.1596(9), 3.1090(5)−3.1439(4), and

Table 4. Selected Interatomic Distances (Å) and Angles (deg) for the Coordination Polyhedra of **I**−**III**[a]

		I	
Ga1−Se1$^{\#1}$	2.3717(15)	Na1−Se1 × 2	3.134(5)
Ga1−Se3$^{\#2}$	2.4247(15)	Na1−Se2 × 2	3.144(5)
Ga1−Se3$^{\#3}$	2.4297(15)	Na1−Se4 × 2	3.208(2)
Ga1−Se2	2.4312(14)	Na1−Se3 × 2	3.260(2)
Ga2−Se2$^{\#4}$	2.3805(15)	Se1$^{\#1}$−Ga1−Se3$^{\#2}$	121.41(5)
Ga2−Se4$^{\#5}$	2.4158(15)	Se1$^{\#1}$−Ga1−Se3$^{\#3}$	119.66(5)
Ga2−Se1$^{\#6}$	2.4269(14)	Se3$^{\#2}$−Ga1−Se3$^{\#3}$	97.75(5)
Ga2−Se4$^{\#7}$	2.4316(15)	Se1$^{\#1}$−Ga1−Se2	101.77(5)
		Se3$^{\#2}$−Ga1−Se2	109.27(5)
La1−Se3 × 4	3.1454(9)	Se3$^{\#3}$−Ga1−Se2	106.20(5)
La1−Se2 × 4	3.1549(10)		
		Se2$^{\#4}$−Ga2−Se4$^{\#5}$	124.65(6)
La2−Se1 × 4	3.1313(10)	Se2$^{\#4}$−Ga2−Se1$^{\#6}$	101.86(5)
La2−Se4 × 4	3.1596(9)	Se4$^{\#5}$−Ga2−Se1$^{\#6}$	102.17(5)
		Se2$^{\#4}$−Ga2−Se4$^{\#7}$	121.89(6)
		Se4$^{\#5}$−Ga2−Se4$^{\#7}$	98.56(5)
		Se1$^{\#6}$−Ga2−Se4$^{\#7}$	104.77(5)
		II	
Ga1−Se1$^{\#1}$	2.3756(7)	Na1−Se1 × 2	3.134(2)
Ga1−Se3$^{\#2}$	2.4258(7)	Na1−Se2 × 2	3.145(2)
Ga1−Se3$^{\#3}$	2.4301(7)	Na1−Se4 × 2	3.2134(8)
Ga1−Se2	2.4348(7)	Na1−Se3 × 2	3.2633(9)
Ga2−Se2$^{\#4}$	2.3792(7)	Se1$^{\#1}$−Ga1−Se3$^{\#2}$	121.18(2)
Ga2−Se4$^{\#5}$	2.4139(7)	Se1$^{\#1}$−Ga1−Se3$^{\#3}$	120.05(2)
Ga2−Se1$^{\#6}$	2.4309(7)	Se3$^{\#2}$−Ga1−Se3$^{\#3}$	97.88(2)
Ga2−Se4$^{\#7}$	2.4367(7)	Se1$^{\#1}$−Ga1−Se2	101.62(2)
		Se3$^{\#2}$−Ga1−Se2	109.64(2)
Ce1−Se3 × 4	3.1312(4)	Se3$^{\#3}$−Ga1−Se2	105.66(2)
Ce1−Se2 × 4	3.1367(5)		
		Se2$^{\#4}$−Ga2−Se4$^{\#4}$	124.89(3)
Ce2−Se1 × 4	3.1090(5)	Se2$^{\#4}$−Ga2−Se1$^{\#6}$	101.96(2)
Ce2−Se4 × 4	3.1439(4)	Se4$^{\#5}$−Ga2−Se1$^{\#6}$	101.62(2)
		Se2$^{\#4}$−Ga2−Se4$^{\#7}$	121.77(3)
		Se4$^{\#5}$−Ga2−Se4$^{\#7}$	98.65(2)
		Se1$^{\#6}$−Ga2−Se4$^{\#7}$	104.92(2)
		III	
Ga1−Se1$^{\#1}$	2.3734(9)	Na1−Se1 × 2	3.129(4)
Ga1−Se3$^{\#2}$	2.4251(10)	Na1−Se2 × 2	3.144(4)
Ga1−Se3$^{\#3}$	2.4270(10)	Na1−Se4 × 2	3.2118(12)
Ga1−Se2	2.4343(10)	Na1−Se3 × 2	3.2652(13)
Ga2−Se2$^{\#4}$	2.3795(10)	Se1$^{\#1}$−Ga1−Se3$^{\#2}$	120.84(4)
Ga2-Se4$^{\#5}$	2.4091(10)	Se1$^{\#1}$−Ga1−Se3$^{\#3}$	120.55(4)
Ga2−Se1$^{\#6}$	2.4279(10)	Se3$^{\#2}$−Ga1−Se3$^{\#3}$	97.83(3)
Ga2−Se4$^{\#7}$	2.4350(10)	Se1$^{\#1}$−Ga1−Se2	101.54(3)
		Se3$^{\#2}$−Ga1−Se2	110.32(3)
Nd1−Se3 × 4	3.1044(6)	Se3$^{\#3}$−Ga1−Se2	104.95(3)
Nd1−Se2 × 4	3.1052(7)		
		Se2$^{\#4}$−Ga2−Se4$^{\#5}$	125.27(4)
Nd2−Se1 × 4	3.0763(7)	Se2$^{\#4}$−Ga2−Se1$^{\#6}$	101.95(3)
Nd2−Se4 × 4	3.1179(6)	Se4$^{\#5}$−Ga2−Se1$^{\#6}$	100.71(3)
		Se2$^{\#4}$−Ga2−Se4$^{\#7}$	121.83(4)
		Se4$^{\#5}$−Ga2−Se4$^{\#7}$	98.71(3)
		Se1$^{\#6}$−Ga2−Se4$^{\#7}$	105.11(3)

[a] Symmetry transformations used to generate equivalent atoms: #1 $x + 3/4, -y + 1, z - 1/4$; #2 $x + 1/4, y - 1/4, -z + 1/2$; #3 $-x + 5/4, -y + 5/4, z$; #4 $x, -y + 5/4, -z + 1/4$; #5 $x - 1/4, y + 1/4, -z + 3/2$; #6 $-x + 3/4, y, -z + 3/4$; #7 $-x + 7/4, -y + 5/4, z - 1/2$.

3.0763(7)−3.1179(6) Å for **I**, **II**, and **III**, respectively. The La−Se, Ce−Se, and Nd−Se distances are in good agreement with the reported values for similar compounds in the literature.[27] There is only one crystallographically unique Na atom in the structure surrounded by eight Se atoms in a square antiprismatic environment. The Na−Se distances are in the range 3.134(5)–3.260(2), 3.134(2)−3.263(1), and 3.129(4)−3.265(1) for **I**, **II**, and **III**, respectively. Each $NaSe_8$

(27) (a) Strobel, S.; Schleid, Th. *J. Alloys Compd.* **2006**, *418*, 80. (b) Hartenbach, I.; Schleid, Th. *J. Alloys Compd.* **2006**, *418*, 95. (c) Strobel, S.; Schleid, Th. *Z. Anorg. Allg. Chem.* **2002**, *628*, 2211.

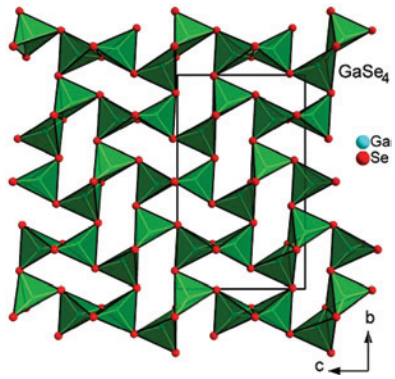

Figure 1. View of the gallium selenide layer along the *a*-axis showing the corner- and edge-sharing of the $GaSe_4$ tetrahedra to create a six-membered aperture within the layer. In the figure the size of the selenium atoms has been reduced to 1/3 of its original.

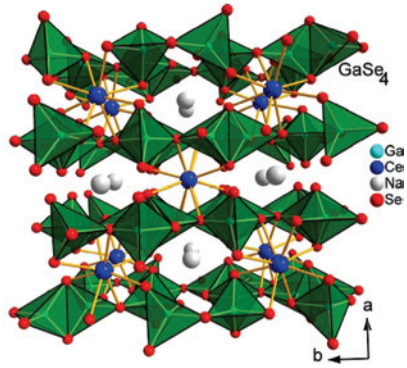

Figure 2. Structure **II** viewed along the *c*-axis, showing how the alkali-metal cations and the lanthanide elements are located between the layers formed by the $GaSe_4$ tetrahedra. In the figure the size of the selenium atoms has been reduced to 1/3 of its original.

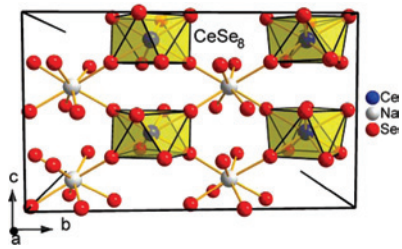

Figure 3. Assembly of $NaSe_8$ and $CeSe_8$ antiprisms viewed along the *a*-axis in the structure of **II** showing that the $CeSe_8$ antiprisms do not share any common apices. The Ga atoms have been omitted in the figure for the sake of clarity and the size of the selenium atoms has been reduced to 1/2 of its original.

polyhedron is connected to four $GaSe_4$ and two $LnSe_8$ units through edge-sharing and to eight $GaSe_4$ and four $LnSe_8$ entities through the vertices. Similar to the $LnSe_8$ case, there are no Na−Se−Na linkages, indicating that the $NaSe_8$ polyhedra are also well-isolated from each other. All four crystallographically distinct Se atoms are tetra-coordinate, surrounded by one Na, one *Ln*, and two Ga atoms, in a distorted tetrahedral environment.

It is interesting to note that compounds **I**−**III** are the only known examples of quaternary stoichiometric seleno-gallates containing rare-earth metals. Moreover, stoichiometric quaternary compounds in the seleno-gallate family are very limited.[28] Though there are several quaternary compounds known in the thio-gallate family, those stoichiometric compounds containing rare-earth metals are also limited.[6c,9e,29] Structurally, compounds **I**−**III** belong to a very robust structure type as exemplified by a large number of variations that the structure can accommodate both in ternary and quaternary compounds. For example, it has been demonstrated that various compounds may be obtained through the variation of the alkaline earth metals, MGa_2S_4 (M = Ca, Sr),[17] the main group elements, MAl_2S_4 (M = Ca, Sr)[17] and MIn_2Q_4 (M = Sr, Ba),[30] the chalcogen elements, $CaGa_2Q_4$ (Q = S, Se),[17,31] both alkaline earth and chalcogen element, MIn_2Q_4 (M = Sr, Ba),[30] as well as other elements (divalent rare-earth metals or Pb^{2+}) in place of the alkaline earth metal, MGa_2S_4 (M = Eu, Yb)[32] and MGa_2Se_4 (M= Pb, Eu).[33] More importantly, one can completely replace the alkaline earth component by an alkali metal and a rare-earth metal simultaneously without any structural change. Three independent sites (8*a*, 8*b*, 16*e*) are occupied by the alkaline-earth metals in the ternaries, $CaGa_2Q_4$ (Q = S, Se),[17,31] two of which (8*a*, 8*b*) can be replaced by one trivalent rare-earth element and one site (16*e*) can be replaced by alkali-metal cations to form a quaternary compound, as shown in the case of the thio-gallate $NaNdGa_4S_8$,[6c] and the three current examples extend this concept to the quaternary seleno-gallate family.

It is very important to be able to tune a property of a material systematically. Such a systematic tuning of properties, for example, the optical property, may be achieved by changing the alkaline earth metal, the chalcogen, or the rare-earth metal. Predictions around subsequent property variations can be done only when the structural integrity is preserved during the change of the element or elements. The robustness of the structure type toward the variation of the elements often simplifies such systematic studies, as is demonstrated in the following optical property study.

Optical Spectroscopy. The reflectance spectra and absorption data calculated using the Kubelka–Munk function for compounds **I**−**III** are shown in Figure 4. The reflectance spectra of all the compounds show strong absorption up to around 400 nm (3.1 eV). The steep absorption edge of $NaLaGa_4Se_8$ (**I**) lies around 2.65 eV, whereas for the compounds **II** and **III**, the same steep transitions are located

(28) (a) Pfeiff, R.; Kniep, R. *J. Alloys Compd.* **1992**, *186*, 111. (b) Krauss, G.; Keller, E.; Kraemer, V. *Z. Kristallogr.* **1996**, *211*, 188. (c) Olekseyuk, I. D.; Gulay, L. D.; Parasyuk, O. V.; Husak, O. A.; Kadykalo, E. M. *J. Alloys Compd.* **2002**, *343*, 125. (d) Ma, H.-W.; Guo, G.-C.; Wang, M.-S.; Zhou, G.-W.; Lin, S.-H.; Dong, Z.-C.; Huang, J.-S. *Inorg. Chem.* **2003**, *42*, 1366. (e) Kienle, L.; Duppel, V.; Simon, A.; Deiseroth, H. J. *Z. Anorg. Allg. Chem.* **2003**, *629*, 443. (f) Hwang, S.-Ju; Iyer, R. G.; Kanatzidis, M. *J. Solid State Chem.* **2004**, *177*, 3640.
(29) (a) Rodier, N.; Guittard, M.; Flahaut, J. *C. R. Acad. Sci., Ser. II* **1983**, *296*, 65. (b) Mazurier, A.; Jaulmes, S.; Guittard, M. *Acta Crystallogr., Sect. C* **1987**, *43*, 1859. (c) Jaulmes, S.; Palazzi, M.; Laruelle, P. *Mater. Res. Bull.* **1988**, *23*, 831.
(30) (a) Klee, W.; Schaefer, H. *Rev. Chim. Miner.* **1979**, *16*, 465. (b) Eisenmann, B.; Hofmann, A. *Z. Kristallogr.* **1991**, *197*, 167.
(31) Klee, W.; Schaefer, H. *Z. Anorg. Allg. Chem.* **1981**, *479*, 125.
(32) (a) Roques, R.; Rimet, R.; Declercq, J. P.; Germain, G. *Acta Crystallogr., Sect. B* **1979**, *35*, 555. (b) Guseinov, G. G.; Mamedov, F. K.; Amiraslanov, I. R.; Mamedov, Kh. S. *Kristallografiya* **1983**, *28*, 866.
(33) (a) Klee, W.; Schaefer, H. *Mater. Res. Bull.* **1980**, *15*, 1033. (b) Rimet, R.; Roques, R.; Zanchetta, J. V.; Declercq, J. P.; Germain, G. *Rev. Chim. Miner.* **1981**, *18*, 277.

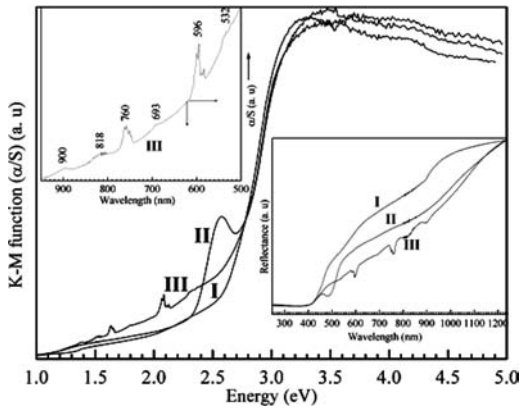

Figure 4. Optical absorption spectra of **I**−**III** transformed from the diffuse reflectance data. Insets on the left top corner is the blow up of the absorption spectra of **III** in the 500–950 nm region to show the $f \rightarrow f$ transition of Nd^{3+}. Inset in the right bottom corner shows the plot of diffuse reflectance spectra of **I**−**III**.

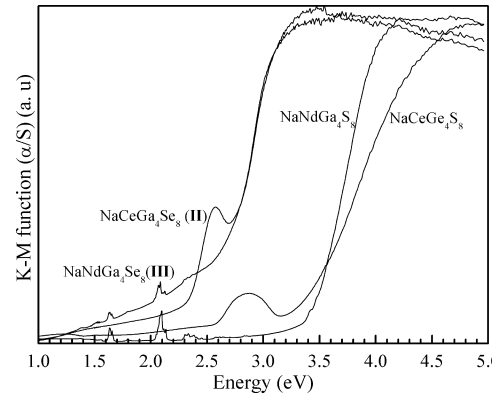

Figure 5. Plot of the optical absorption spectra of **II** and **III** along with their isostructural thio-analogues, $NaCeGa_4S_8$ and $NaNdGa_4S_8$, to show the variation of absorption spectra of the lanthanides from the sulfide to selenide environment in isostructural compounds.

around 2.66 and 2.73 eV, respectively. In the absence of any f and d electrons (La^{3+} ($4f^0$, $5d^0$)), the transition at 2.65 eV for **I** can be assigned to the electronic transition from predominantly valence band (VB) to the conduction band (CB) of the host. The top of the VB can be assumed to form from the predominantly anionic (Se^{2-}) orbitals and also hybridization of Se(4p) electrons with Ga(4s) and Ga(4p) electrons to form the Ga−Se bonds will also constitute part of VB. The bottom of CB can be assumed to be made of predominantly La-5d orbitals, whereas Ga−Se antibonding orbitals, with Ga(4s) and Ga(4p) electrons will also form higher energy levels of CB. The empty *Ln*-5d levels are formed below the CB as described in the energy level diagrams for $CaGa_2S_4$:*Ln*,[11f,i] whereas, the lanthanide *f*-energy levels are located below the CB and above the VB (for Ce) or spreads around the occupied levels of the VB (for Nd). Similar assignment energy levels has been done previously in rare-earth metal containing isostructural thio-gallates[6b,d,9e,11f,i] as well as from theoretical calculations.[34] The VB → CB transition (band gap) is expected to be located at a similar energy threshold in both Ce- and Nd-containing compounds because the anionic and cationic orbitals are basically the same, however, a little increase of VB → CB gap is expected with the decreasing size of rare-earth metals. So the steep transitions around 2.66 and 2.73 eV for **II** and **III**, respectively, are also due to VB → CB. A second absorption threshold in the case of **II**, beginning at around 2.32 eV and having a maximum at 2.57 eV, can be attributed to the 4f-5d intra-atomic Ce transition, as has also been observed in the thio-analogue.[9e] On the other hand, several absorptions characteristic of the Nd^{3+} transition ($^4I_{9/2} \rightarrow {}^{2S+1}L_j$) are observed between 800 - 530 nm before the interband transition of **III**. These transitions can be tentatively assigned with the help of previous reports and they originate from the ground state $^4I_{9/2}$ to $^2K_{13/2} + {}^4G_{7/2,9/2}$ (532 nm), $^4G_{5/2} + {}^2G_{7/2}$ (596 nm), $^4H_{11/2}$ (635 nm, very weak), $^4F_{9/2}$ (693 nm), $^4F_{7/2} + {}^4S_{3/2}$ (760 nm), $^2H_{9/2}$, $^4F_{5/2}$ (818 nm), and $^4F_{3/2}$ (900 nm).[15b] The similarity of the color of the powdered samples of **I** and **II** indicates that the origin of that color is due to the charge transfer from VB to CB; a darker color for **III** is probably caused by a little higher band gap (2.73 eV) of the compound. Preliminary luminescence property investigations indicate that **II** and **III** are not luminescent at room temperature.

It would be very interesting to compare and contrast the absorption spectra of **II** and **III** to their sulfide analogues. Such a comparison will allow us to precisely demonstrate how the optical properties vary both in terms of the parity forbidden f → f and parity allowed f → d transitions of the lanthanide cations on changing from sulfide to selenide in isotypic compounds. For this purpose, we have synthesized $NaCeGa_4S_8$ and $NaNdGa_4S_8$, employing a new synthetic strategy. A quick glance at Figure 5 reveals that there is a substantial narrowing of the band gap from 3.41 and 3.45 eV for $NaCeGa_4S_8$ and $NaNdGa_4S_8$, respectively, to 2.66 and 2.73 eV in the respective selenide analogues (**II** and **III**). This decrease of about 0.72–0.75 eV in the band gap (VB → CB transition) is obvious as the energy level of Se(4p) orbitals, which is expected to contribute to the valence band, lie higher in energy than S(3p) orbitals. The $4f^1 \rightarrow 5d$ transition energy of Ce^{3+} also shows a variation in the sulfide from the selenide; the $4f^1 \rightarrow 5d$ threshold lies at 2.58 eV with a maximum at 2.87 eV (432 nm) and a broader peak of $4f^1 \rightarrow 5d$ transition is observed for the sulfide.

It should be noted that $NaCeGa_4S_8$ is highly luminescent at room temperature (see the Supporting Information, Figure S2) and the scattered emitted light will affect the absorption spectra collected in a Praying Mantis accessory without the use of a background monochromator. This modification will take place at the high-energy end of the emission peak (starting at 440 nm, 2.81 eV) and will affect the $4f^1 \rightarrow 5d$ transition threshold. Thus, the $4f^1 \rightarrow 5d$ transition threshold is shifted toward lower energy and also the peak is broadened. Nevertheless, a shift toward the lower energy by 0.26 eV (which is underestimated) in **II**, could be due to the increased covalency raising the f-level energy and causing a higher dispersion of the Ce-5d level resulting in a lowering of the Ce-5d band.[14a] As the covalency increases, the increase in the f-orbital energy is caused by a larger screening effect of the nucleus by the higher concentration of valence

(34) Nomura, S.; Takizawa, T.; Endo, S *J. Phys. Chem. Solids* **2005**, *66*, 2090.

electrons around the cation.[16] On the other hand, the parity forbidden f → f transitions of Nd^{3+} are less affected by the type of chalcogen, as the f orbitals are deeply seated. However, there is a small shift of the f → f transition to lower energy in **III** (by 5 – 7 nm) due to the nephelauxetic effect caused by higher degree of covalency, which leads to the expansion of the partially filled 4f-shell decreasing the repulsion within the 4f-shell of rare-earth metal cations.[35]

The energy levels of the lanthanide orbitals in the energy band structure of a semiconductor depend on the composition of the anionic environment of the lanthanide (that is, on the chemical composition of the first coordination sphere). Isostructural chalcogenides thus provide a variation in the composition of the anionic sublattice, which can incorporate S or Se. This property allows a directed change in energy-level positions of lanthanide centers in the energy band structure of the semiconductor.

Conclusions

We have successfully synthesized two new quaternary seleno-gallates containing rare-earth elements and determined their structures. The location of the rare-earth elements in the structures is the same as that in the isostructural $NaNdGa_4S_8$. This work also demonstrates that it is possible to tune the optical properties of materials by simply changing the anionic environment of the rare-earth element in isostructural compounds. We are currently investigating the low-temperature luminescence properties of these two compounds to accomplish the excitation of lanthanide energy levels and show the importance of the location of lanthanide energy levels in the energy band structure.

Acknowledgment. The authors acknowledge financial support provided by the National Science Foundation, NSF-DMR-0343412.

Supporting Information Available: X-ray crystallographic data in CIF format for **I**−**III** and figures containing the color photograph for compounds, $NaCeGa_4S_8$, $NaNdGa_4S_8$, **II**, and **III** (Figure S1) and PL spectra of $NaCeGa_4S_8$ (Figure S2) (PDF). The material is available free of charge via the Internet at http://pubs.acs.org.

IC701986J

(35) Jorgensen, C. K. *Modern Aspects of Ligand Field Theory*; North-Holland: Amsterdam, 1971.